4-23-2015

Quantifying the Sensitivity of Maximum, Limiting, and Potential Tropical Cyclone Intensity to SST: Observations Versus the FSU/ COAPS Global Climate Model

Sarah Strazzo
Embry-Riddle Aeronautical University, Sarah.Strazzo@erau.edu

James Elsner
Florida State University

Tim LaRow
Florida State University

Scholarly Commons Citation

Strazzo, S.E., J.B. Elsner, and T.E. LaRow(2015),Quantifying the sensitivity of maximum, limiting, and potential tropical cyclone intensity to SST: Observations versus the FSU/COAPS global climate model, J.Adv.Model.EarthSyst.,7,586–599, doi:10.1002/2015MS000432.

AGU PUBLICATIONS

Journal of Advances in Modeling Earth Systems

RESEARCH ARTICLE

10.1002/2015MS000432

Key Points:
- Link statistical TC limiting intensity to theoretical TC potential intensity
- Quantify differences in observed/simulated sensitivities of TC intensity to SST
- Understand why GCMs miss the sensitivity of hurricane limiting intensity to SST

Correspondence to:
S. E. Strazzo,
ses09e@my.fsu.edu

Citation:
Strazzo, S. E., J. B. Elsner, and T. E. LaRow (2015), Quantifying the sensitivity of maximum, limiting, and potential tropical cyclone intensity to SST: Observations versus the FSU/COAPS global climate model, *J. Adv. Model. Earth Syst.*, *7*, 586–599, doi:10.1002/2015MS000432.

Received 23 JAN 2015
Accepted 18 MAR 2015
Accepted article online 24 MAR 2015
Published online 23 APR 2015

Quantifying the sensitivity of maximum, limiting, and potential tropical cyclone intensity to SST: Observations versus the FSU/COAPS global climate model

S. E. Strazzo[1], J. B. Elsner[1], and T. E. LaRow[2]

[1]Department of Geography, Florida State University, Tallahassee, Florida, USA, [2]Department of Earth, Ocean, and Atmospheric Sciences, Center for Ocean-Atmospheric Prediction Studies, Florida State University, Tallahassee, Florida, USA

Abstract Previous research quantified the sensitivity of limiting intensity to SST for observed tropical cyclones (TCs) and for TCs generated by two global climate models (GCMs). On average, a 1° C increase in sea surface temperature (SST) is associated with a 7.9 m s^{-1} increase in the statistical upper limit of observed intensity. Conversely, a 1°C increase in SST does not significantly affect the limiting intensity of GCM-generated TCs. The study presented here builds on previous research in two ways: (1) A comparison is made between the statistically defined limiting intensity and the physically defined potential intensity, and (2) a test is performed on the ability of a ∼0.94° resolution GCM to reproduce the observed statistical relationship between potential intensity and SST. Data from NASA's Modern Era Reanalysis are used to approximate the observed sensitivity of potential intensity to SST for the 1982–2008 time period. Results indicate that the sensitivity of potential intensity to SST is not statistically different from the sensitivity of observed maximum or limiting intensity to SST. This result links the statistically defined sensitivity to the physically based theory of hurricanes. Potential intensity is also estimated from the FSU/COAPS GCM. Although the FSU/COAPS model does not capture the observed sensitivity of TC maximum or limiting intensity to SST, the model reproduces the observed sensitivity of potential intensity to SST. The model generates suitable atmospheric conditions for the development of strong TCs, however strong TCs do not develop, possibly as a result of insufficient resolution.

1. Introduction

Given the rise in ocean heat content and sea surface temperature (SST) observed during the second half of the 20th century [*Levitus et al*., 2000, 2012], numerous studies seek to understand how increasing SSTs might affect tropical cyclones (TCs), both in terms of frequency and intensity [e.g., *Emanuel*, 1987; *DeMaria and Kaplan*, 1994; *Emanuel*, 2005; *Elsner et al*., 2008; *Knutson et al*., 2008; *Bender et al*., 2010; *Kunkel et al*., 2013; *LaRow et al*., 2014]. The effects of climate change on TC frequency remain uncertain, with some research suggesting decreases in overall North Atlantic TC numbers [e.g., *Zhao et al*., 2009; *Held and Zhao*, 2011] and others suggesting increases [e.g., *Emanuel*, 2013]. Despite this uncertainty about changes in TC frequency, many observational and modeling studies support the notion that increasing SSTs should lead to more intense TCs, although some studies suggest that this signal only exists in the set of the strongest TCs [*Elsner et al*., 2008; *Bender et al*., 2010].

Although much of this research focuses on the relationship between increasing SSTs and various metrics of TC activity, *Kunkel et al*. [2013] caution that SST is not an ideal proxy for the thermodynamic environment of TCs. They note that TC potential intensity is a function of the degree of thermodynamic disequilibrium between the atmosphere and upper ocean and that this disequilibrium does not depend on SST alone, but rather on the difference between the temperature near the sea surface and the temperature throughout the depth of the troposphere [*Emanuel*, 1995]. In fact, *Emanuel et al*. [2013] quantify the theoretical direct effect of SST on potential intensity as a mere 0.4 m s^{-1} increase in potential intensity for a 1.0°C increase in SST. Furthermore, additional environmental variables (e.g., tropopause temperature, vertical shear of the horizontal winds, and midlevel relative humidity) are thought to influence TC intensity [e.g., *DeMaria*, 1996; *Wong and Chan*, 2004; *Braun et al*., 2012; *Emanuel et al*., 2013].

Nevertheless, research shows that TC intensity is statistically related to SST. For example, *Merrill* [1987] demonstrates that stronger TCs tend to occur over warmer ocean water, although they note that higher SSTs alone could not be used to predict intensity or intensification. Similarly, *DeMaria and Kaplan* [1994] bin climatological SSTs at 1°C intervals and find a generally positive but nonlinear empirical relationship between these binned SSTs and maximum TC intensity. The strongest relationship exists for TCs occurring over water with temperatures greater than 26°C. *Elsner et al.* [2008] employ quantile regression to highlight the strong positive relationship between SST and TCs with intensities in the upper quantile of the climatological TC intensity distribution. Additionally, *Emanuel* [2005] examines TC power dissipation—a measure of the destructive potential of a TC expressed as a function of the cubed wind speed integrated over storm lifetime—and find a strong, statistically significant relationship between power dissipation and SST.

Building on this earlier research, *Elsner et al.* [2012b] approach the problem using the spatial tessellation framework first introduced in *Elsner et al.* [2012a]. They divide the North Atlantic basin into a tessellation of equal-area hexagons onto which TC track point data and gridded SST data are both overlaid. For each hexagon (i.e., region), *Elsner et al.* [2012b] use extreme value theory to statistically model the upper limit of TC intensity from the set of per TC maximum intensities for that region. They then regress the per hexagon limiting intensity values onto the set of per hexagon August–October average SSTs to obtain an estimate of the sensitivity of limiting intensity to SST. They consider only those regions with SSTs exceeding 25°C and find that a 1°C increase in SST is associated with a 7.9 ± 1.19 m s^{-1} increase in per hexagon limiting intensity.

In addition to these observation-based studies, many global climate model (GCM) and downscaled simulations of 21st century TC activity similarly predict increasing TC intensity under various climate change scenarios, particularly for the most intense TCs [e.g., *Emanuel*, 2013; *Knutson et al.*, 2013; *Villarini and Vecchi*, 2013]. Although some of these studies circumvent insufficient resolution issues through statistical and/or dynamical downscaling techniques, it should be noted that because GCM resolution is still too coarse to resolve key TC features [e.g., *Chen et al.*, 2007], these results must be considered with some caution. In fact, *Elsner et al.* [2013] use the same spatial framework and limiting intensity model as *Elsner et al.* [2012b] to show that two medium resolution GCMs—the FSU/COAPS model and the GFDL-HiRAM—do not reproduce the observed sensitivity of TC limiting intensity to SST. The inability of these GCMs to simulate TCs with intensities exceeding ~50 m s^{-1} likely limits the ability of such models to capture the sensitivity. *Elsner et al.* [2012b] speculate that the inability of GCMs to resolve the TC inner core thermodynamics prevent simulated TCs from operating as an idealized heat engine, although this hypothesis has yet to be tested.

The current study builds upon previous research by first examining the link between the sensitivity of the statistical limiting intensity to SST and the sensitivity of the theoretical potential intensity to SST. Because we focus on the most intense TCs (i.e., those TCs we expect to be closer to their potential intensity on average), we anticipate very little difference between sensitivity values for limiting intensity and sensitivity values for the theoretical potential intensity. Examining the sensitivity of potential intensity to SST also provides another metric with which to assess GCM performance. It has already been established that GCMs with horizontal resolution in the 50–100 km range are unable to capture the sensitivity of observed TC limiting intensity to SST; however, whether this discrepancy can be largely explained by insufficient model resolution remains to be explored. Although such GCMs neither capture the observed distribution of TC intensity nor the sensitivity of TC maximum and limiting intensity to SST, we now ask whether they successfully reproduce the observed sensitivity of *potential intensity* to SST. For consistency with previous research, this study applies the same spatial tessellation framework used in *Elsner et al.* [2012b] and *Elsner et al.* [2013]. The remainder of the paper will proceed as follows: section 2 introduces the data sets used, section 3 describes the spatial framework and statistical methods applied, sections 4 and 5 present the results, and section 6 provides a summary and discussion.

2. Data

This research relies on observed, modeled, and reanalyzed data for the period 1982–2008. We consider this period because it matches the period covered by a historical simulation by the FSU/COAPS climate model. Observed TC track data come from the National Hurricane Center's best-track data set, which provides information on TC center location, 1 min wind speed at 10 m above the surface, and minimum central pressure

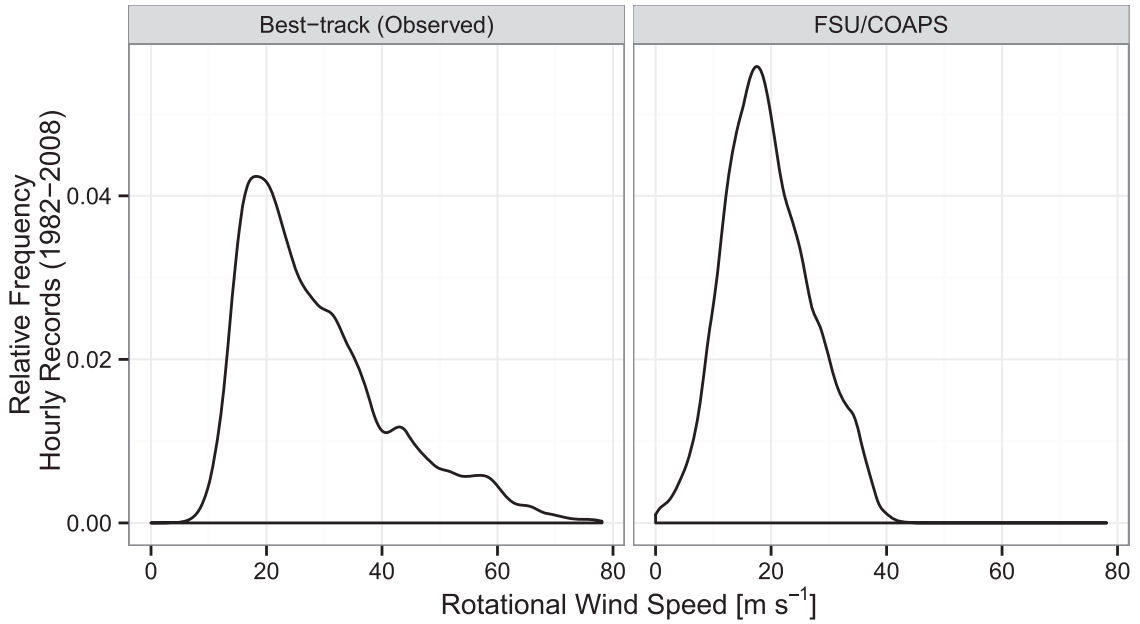

Figure 1. Wind speed relative frequency distributions for best-track (observed) and FSU/COAPS model-generated TCs. Wind speed is shown in units of m s^{-1}.

for all known North Atlantic TCs [*Jarvinen et al*., 1988]. Over the 1982–2008 period, best-track (observed) data are recorded at 6 hourly intervals. Because this analysis requires a higher temporal resolution, we interpolate the 6 hourly observations to obtain hourly data. The interpolation method, described in detail by *Elsner and Jagger* [2013], uses a spline technique that preserves TC attribute values at the 6 hourly intervals and applies a piecewise polynomial function to estimate the hourly wind speeds and pressures between observations. The algorithm similarly preserves TC location at the 6 hourly intervals and uses spherical geometry to obtain the interpolated hourly positions.

In addition to observed TC data, we examine model-generated TCs and atmospheric fields from the Florida State University/Center for Ocean-Atmospheric Prediction Studies (FSU/COAPS) global climate model [*Cocke and LaRow*, 2000; *LaRow et al*., 2008]. Model data come from a historical simulation that was developed as part of a series of experiments by the U.S. Climate Variability and Predictability Research Program (CLIVAR) Hurricane Working Group [*Walsh et al*., 2015]. The version of the FSU/COAPS model used here is not coupled to an ocean model but is instead forced with prescribed SSTs from the Hadley Center Sea Ice and Sea Surface Temperature (HadISST) data set [*Rayner et al*., 2003]. The model was run with 27 vertical levels and a horizontal resolution of T126 ($\sim$0.94° latitude). *LaRow et al*. [2008] describe the algorithm used to detect and track TCs in the model fields. The algorithm searches for a spatially and temporally coinciding vorticity maximum, sea level pressure minimum, and midlevel temperature maximum. It should be noted that, unlike the observed data, model-generated TCs must persist for a minimum of 2 days to be included in the model data record. Additionally, the model data set only includes TCs with lifetime maximum wind speeds of at least 17 m s^{-1}. Therefore, we similarly consider only those observed TCs with maximum wind speeds of at least 17 m s^{-1}. The distributions of hourly observed and modeled wind speeds have similar shapes (Figure 1), although the observed wind speeds have a longer right tail. Modeled wind speeds do not exceed 45 m s^{-1}. In fact the highest wind speed of any model-generated TC is 44.1 m s^{-1} (Table 1). In contrast, the highest wind speed of any observed TC is 78.1 m s^{-1}.

To estimate the sensitivity of TC intensity to SST, we utilize version 3b of NOAA's extended reconstructed SST (ERSST) data set [*Smith et al*., 2008]. The ERSST data are provided on a 2° by 2° grid and do not include any satellite-derived values. Additionally, we approximate observed potential intensity using gridded reanalysis data from NASA's Modern Era ReAnalysis [MERRA; *Rienecker et al*., 2011] maintained by the Global Modeling and Assimilation Office. The MERRA product provides reanalyzed atmospheric data on a 1.25° by 1.25° grid for the period beginning in 1979. Using monthly means of MERRA sea level pressure,

Table 1. Basic Descriptive Statistics for Observed and Model-Generated (FSU/COAPS) TCs[a]

	Observed	FSU/COAPS
Total TCs	314	382
Min wind speed (m s^{-1})	4.88	2.67×10^{-3}
Max wind speed (m s^{-1})	78.1	44.1
Mean wind speed (m s^{-1})	28.8	19.5

[a]"Total TCs" represent the total number of observed or model-generated TCs over the 1982–2008 time period. Maximum (Max), minimum (Min), and mean TC wind speeds are presented with units of m s^{-1}. Note that this table describes the entire sets of observed and modeled raw TC data. The remaining analysis focuses on only those observed and model-generated TCs with maximum wind speeds that exceed 17 m s^{-1}.

relative humidity (converted to mixing ratio), and temperature fields, we compute mean potential intensity values at grid points. To be consistent with the model data, we calculate the monthly means from daily 12 UTC data. Although we acknowledge that reanalysis products do not represent real atmospheric observations, these data nevertheless provide approximate historical atmospheric conditions at the relatively high spatial and temporal resolutions that this analysis requires. Relative to the NCEP-NCAR reanalysis, which *Vecchi et al*. [2013] and *Kossin* [2015] suggest contains spurious negative trends in upper troposphere and tropopause temperature, the MERRA product features higher vertical and horizontal resolution, making it a more suitable option for this analysis.

3. Methods

3.1. Spatial Tessellation

While many previous studies considered relationships between TC intensity and SST by examining paired values of observed SST and TC wind speed [e.g., *Evans*, 1993], here we instead rely on the spatial tessellation approach applied in *Elsner et al*. [2012b] and *Elsner et al*. [2013]. This choice is made primarily because the method allows us to easily employ statistical techniques to examine and display relationships between TC intensity and SST. Importantly, it facilitates the use of extreme value theory to estimate TC limiting intensity. We begin by dividing the North Atlantic basin into equal area hexagon regions. The selection of hexagons is made following results presented in *Elsner et al*. [2012a] that demonstrate that hexagons more efficiently cover TC track data. Particularly for curved tracks, it takes fewer hexagons to cover a TC track compared to rectangles of the same size. For consistency, we refer to these hexagons as "regions." Each region has an area of 731,935.3 km^2, which is slightly larger than the U.S. state of Texas.

Next, we overlay TC track data onto the regions (Figure 2). Both observed and model-generated data are overlaid onto the same set of regions to facilitate comparison. Per region observed and model-generated TC counts are calculated as the total number of observed or simulated TCs to pass over a given region. For the analysis of observed TC data, we only consider regions with at least 15 observed TCs. Similarly, we only consider regions with at least 15 model-generated TCs for the analysis of model data. We set this threshold of 15 TCs per region to ensure that there are sufficient data to generate a statistical model for limiting intensity, as described in the following section. Note that because the spatial distribution of model-generated TCs does not match that of observed TCs, the specific regions used for the analysis of observed TCs do not necessarily match those used for the analysis of model-generated TCs. For example, several of the regions covering the Gulf of Mexico are not included in the analysis of model-generated data as a result of the lack of model-generated TC activity over this portion of the basin. The base tessellation of regions onto which the data are overlaid is the same, but the specific regions used for the analysis varies for model-generated versus observed data. Overall, the model does a reasonable job at generating and tracking TCs over regions where observed TCs occur across the North Atlantic basin (Figure 2). However, the frequency of model-generated TCs across the south-central portion of the basin exceeds that of the observations by a wide margin. Conversely, the model forms and tracks far fewer TCs than are observed over the Gulf of Mexico, as discussed previously in *Strazzo et al*. [2013a].

Finally, we overlay gridded SST data onto the same regions and average the values from August through October over the period 1982–2008 (Figure 3). The warmest August–October SSTs occur south and west in the basin. A visual comparison of the spatial patterns of SST and maximum TC intensity suggests that the highest intensity TCs occur over areas with highest SST. In contrast, regions with the most intense model-generated TCs do not necessarily correspond to regions with the highest SST. We quantify this statistical relationship between per region maximum intensity and SST and compare it to potential intensity in section 5.

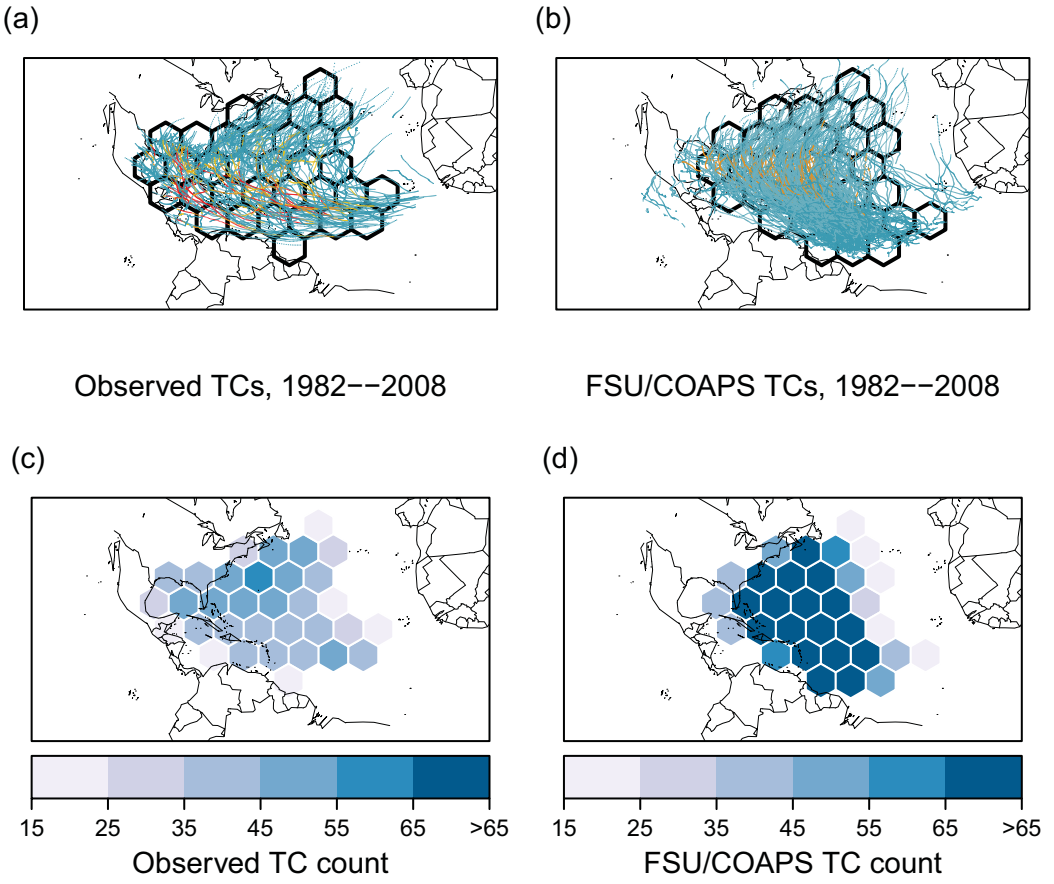

Figure 2. All observed (a) and modeled (FSU/COAPS; b) TC tracks from the 1982–2008 period overlaid onto the same tessellation of equal-area hexagons. Tracks are shaded in proportion to TC category on the Saffir-Simpson scale with blues representing tropical storms and reds representing strong hurricanes. Figures 2c and 2d display per region TC counts for observed and modeled TCs, respectively. Only regions with at least 15 observed TCs (Figures 2a and 2c) or 15 model-generated TCs (Figures 2b and 2d) are displayed.

3.2. Limiting and Potential Intensity

We next calculate limiting and potential intensity. Limiting intensity is a statistical upper limit on per region TC maximum intensity. We estimate limiting intensity for a given region using the climatology of per TC maximum intensities over that region. For each region with a TC count of at least 15, a generalized Pareto distribution is used to describe the set of all TC maximum wind speeds that exceed some threshold value. The generalized Pareto distribution is an extreme value distribution used to model exceedances over a threshold, u. For each region, we define the threshold as the 52nd percentile from the set of per TC maximum wind speeds over that region. The selection of a threshold is relatively subjective. We select our threshold as a balance between (a) the need for sufficient data from which to generate a statistical model, and (b) the requirement that the data be adequately described by extreme value statistics (i.e., the data lie in the tails of the distribution).

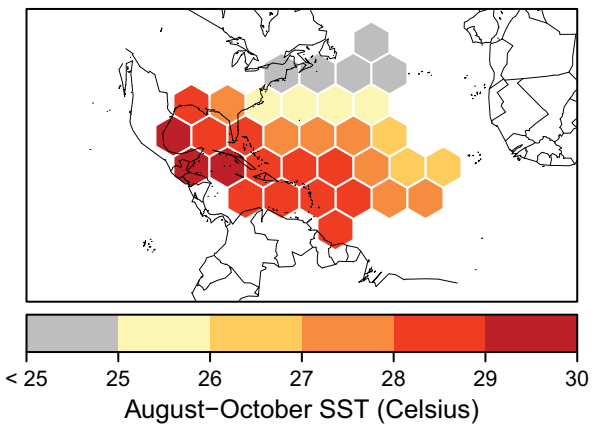

Figure 3. Per region average August–October SST over the 1982–2008 time period. Units are given in °C. Only regions with at least 15 observed TCs are displayed. Gray shading indicates regions with average August–October SST < 25°C.

The generalized Pareto distribution is characterized by two model parameters, the

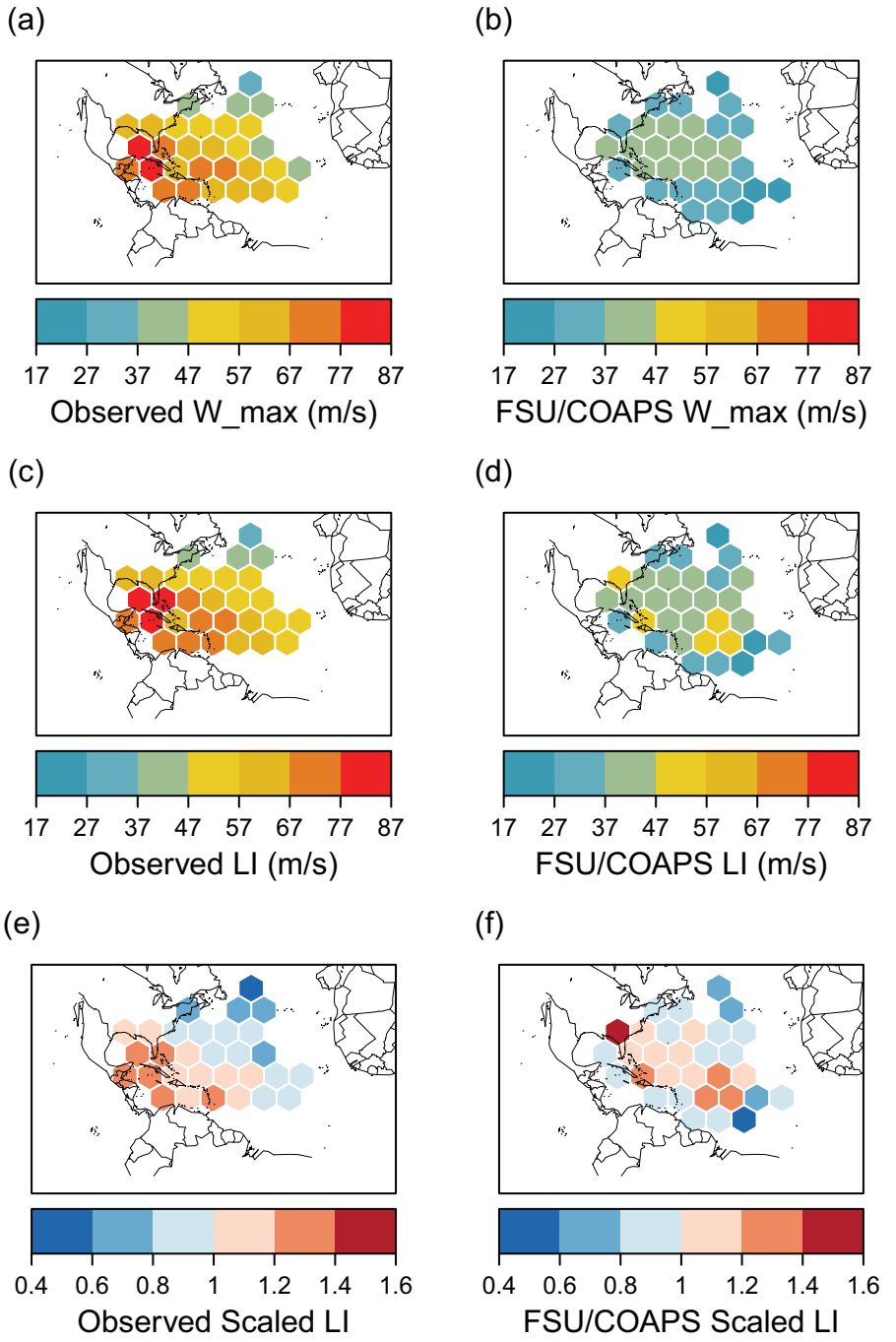

Figure 4. Per region maximum intensity (W_max) from observed (a) and model-generated (FSU/COAPS; b) TCs. Figures 4c and 4d display the per region limiting intensities (LI) estimated from observed and modeled data, respectively. Figures 4e and 4f depict per region limiting intensity scaled by the basin-wide mean per region limiting intensity using observed and model-generated data, respectively. Scaled values less than 1 indicate limiting intensity below the basin wide average, while values greater than 1 indicate limiting intensity above the basin wide average. Limiting and maximum intensities are expressed in units of m s^{-1}.

shape parameter (ξ) and the scale parameter (σ), which we obtain using maximum likelihood estimation. For $\xi < 0$, the probabilities decrease to zero above a certain wind speed. For these cases, we define the upper limit of wind speed to be the limiting intensity, expressed as:

$$\text{Limiting intensity} = u - \sigma/\xi \tag{1}$$

Because the regions are generally data sparse, the method sometimes underestimates the per region limiting intensity, as described in *Strazzo et al.* [2013b]. As additional TCs are added to the database in time, this

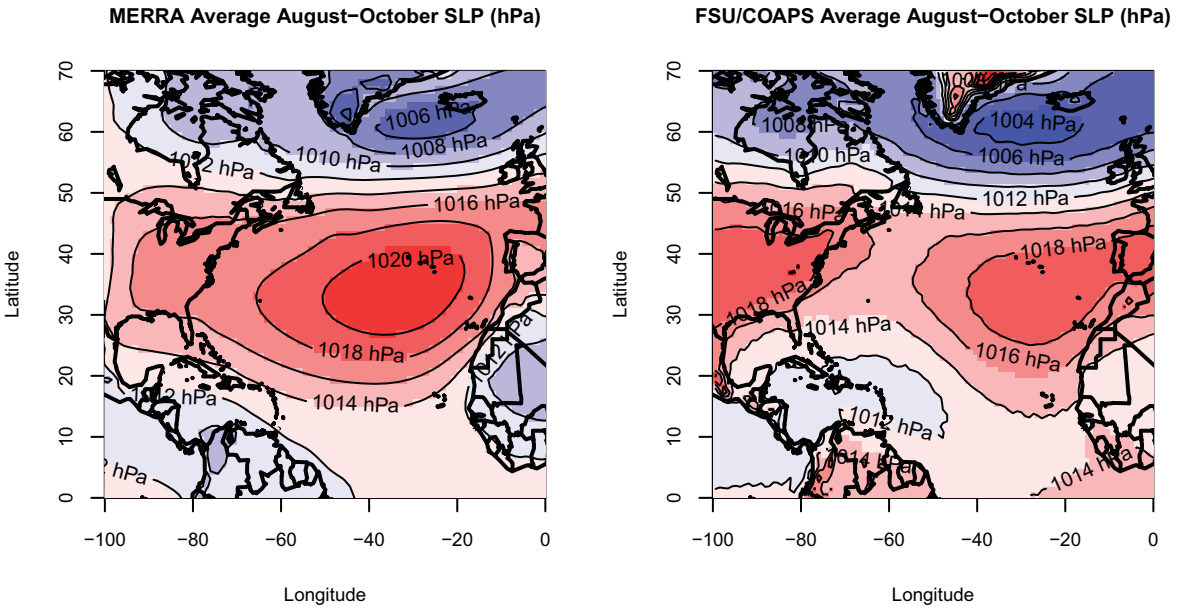

Figure 5. Mean August–October sea level pressure (SLP) data from MERRA (left) and the FSU/COAPS model (right) over the 1982–2008. Contouring is shown at 2 hPa intervals.

problem should subside. Using this method, we compute per region limiting intensity for both observed and model-generated TCs.

In addition to the statistical limiting intensity, we calculate the per region potential intensity, where potential intensity is defined as the maximum intensity a TC could theoretically attain in a specific thermodynamic environment [*Emanuel*, 1995]. We use Kerry Emanuel's algorithm (available from ftp://texmex.mit.edu/pub/emanuel/TCMAX/), translated to the R language by Thomas Jagger. The algorithm estimates potential intensity from the vertical profile of atmospheric temperature, mixing ratio, and pressure for a given location. Because we do not have a set of observed atmospheric data for the time period and region of interest, we estimate monthly potential intensity from the set of monthly gridded MERRA atmospheric data. We similarly compute monthly potential intensity from FSU/COAPS monthly mean atmospheric data. The gridded potential intensity data are subsequently overlaid onto the same set of regions, as was done for TC and SST data. This allows us to compute per region potential intensity, which we define as the highest potential intensity over a given region during the 1982–2008 time period. Section 4 compares regional values of maximum, limiting, and potential intensity for observed/reanalyzed and modeled data.

4. Spatial Patterns of Maximum, Limiting, and Potential Intensity

We next examine per region maximum and limiting intensities for observed and model-generated TCs (Figure 4). Per region maximum intensity represents the maximum TC intensity that occurred over that region during the 1982–2008 time period. Per region limiting intensity is calculated as described in section 3.2. As before, we use the same set of regions for our comparison but only consider regions that have at least 15 observed or model-generated TCs. Additionally, we remove regions for which the shape parameter (ξ) from the limiting intensity model is greater than zero. For these regions, a limiting intensity does not exist, likely because of too few data. In total, four regions were removed for this reason.

As expected, the maximum and limiting intensities of model-generated TCs are significantly less than those of observed TCs (Figure 4). The strongest observed TCs, some of which reach intensities exceeding 70 m s^{-1}, tend to occur over the Gulf of Mexico, while the strongest model-generated TCs occur over the central Atlantic and do not intensify beyond $\sim$45 m s^{-1}. This pattern also exists for limiting intensity. Because per

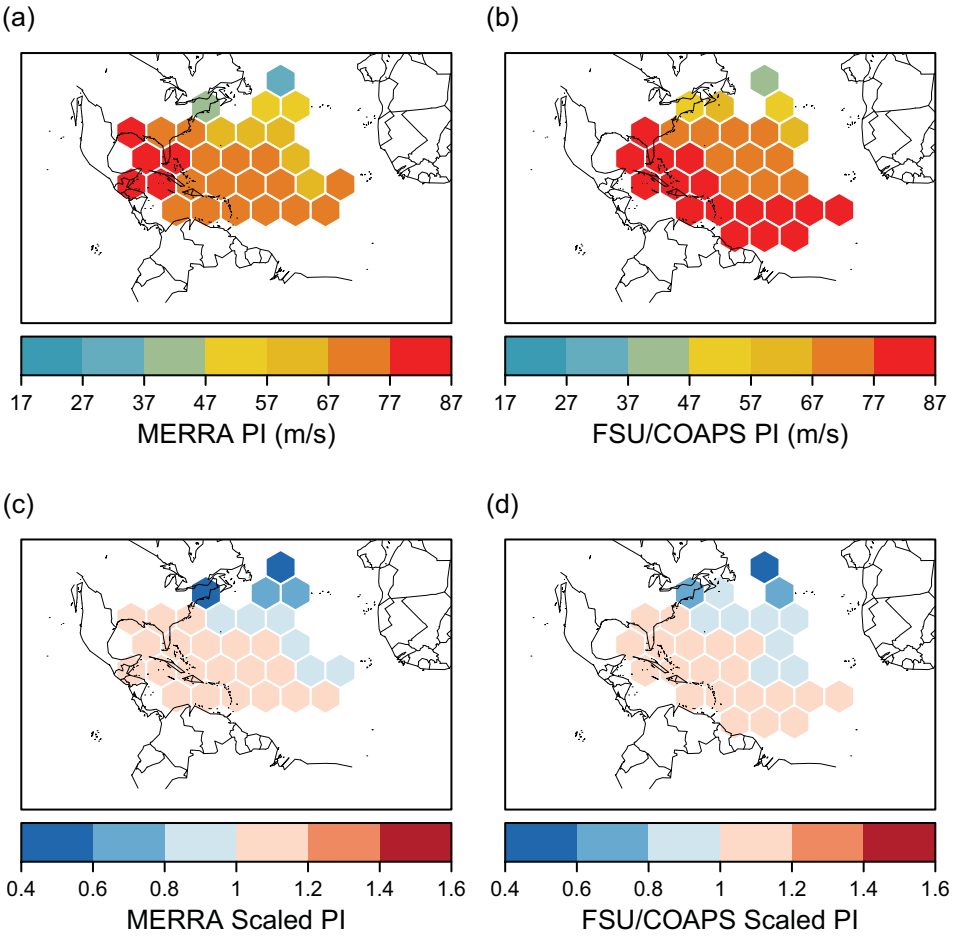

Figure 6. Observed (MERRA; a) and modeled (FSU/COAPS; b) per region potential intensity. Figures 6c and 6d depict potential intensity scaled by the mean per region potential intensity for observed (MERRA; c) and modeled (FSU/COAPS; d) data. Scaled values less than 1 indicate per region potential intensity below the basin wide average, while values greater than 1 indicate per region potential intensity above the basin wide average. Potential intensity is expressed in units of m s^{-1}.

region limiting intensity of model-generated TCs is estimated from the climatology of modeled TC maximum wind speeds, it is reasonable that the FSU/COAPS limiting intensities are not as high as those estimated from the observed TC climatology. To better visualize the difference in the spatial distribution of observed and modeled limiting intensity, we scale each per region limiting intensity by the average per region limiting intensity (Figure 4). Regions with the highest observed and simulated limiting intensities do not match. Overall, weaker observed TCs occur over the eastern and northern portions of the basin, as we would expect. However, regions with the most intense model-generated TCs occur farther east in the basin relative to observations.

As noted in *LaRow et al.* [2008] and *Strazzo et al.* [2013a], relatively few model-generated TCs occur over the Gulf of Mexico compared to what we observed over the same time period. This may be partially explained by a lack of modeled TC genesis over this region [*Strazzo et al.*, 2013a]. Additionally, *LaRow et al.* [2008] remark that, compared to observations, a higher percentage of FSU/COAPS TCs recurve prior to reaching the Caribbean and Gulf of Mexico. This results from differences in typical observed and modeled August–October sea level pressure patterns over the North Atlantic. The FSU/COAPS model places a weaker Bermuda High farther east in the basin relative to the pattern present in the MERRA reanalysis (Figure 5). A weakness in the ridge over the North Atlantic helps steer model-generated TCs that form over the central Atlantic northward before reaching the Gulf of Mexico. This pattern may partially explain the eastward displacement of the highest model-generated TC intensities relative to observations. Model-generated TCs form in the main development region and initially track northwestward and intensify before reaching the midlatitude westerlies and cooler SSTs. While model resolution likely limits the ability of the FSU/COAPS

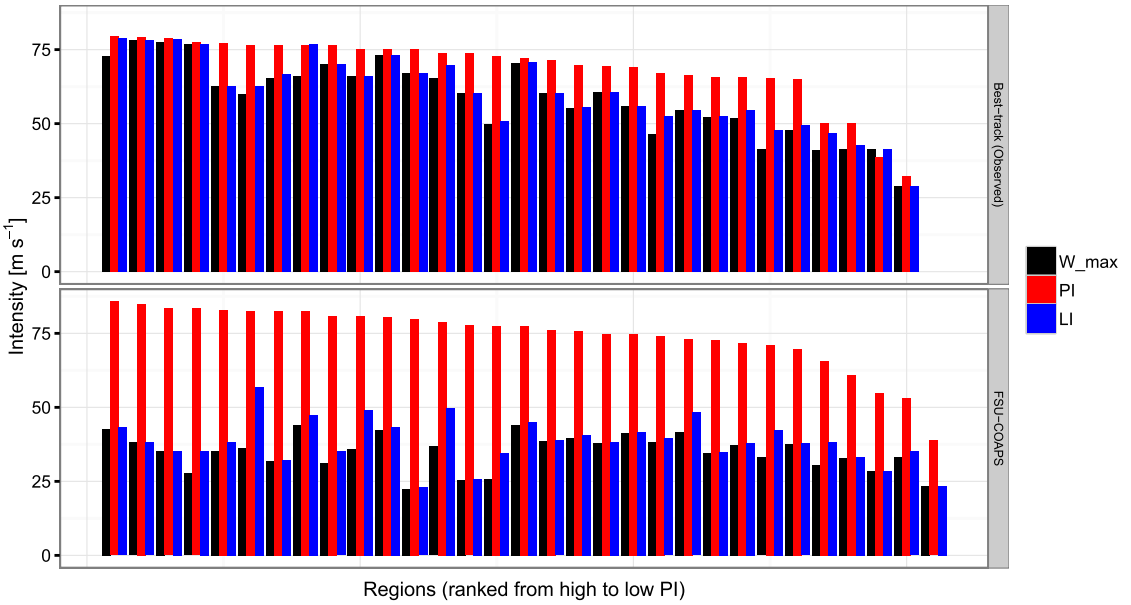

Figure 7. A comparison of per region maximum, potential, and limiting intensity for observed (top) and model-generated (bottom) TCs. Each set of three bars represents the maximum (black), limiting (blue), and potential (red) intensity for a specific region. Regions are presented in descending order from those of highest to lowest potential intensity. Maximum, limiting, and potential intensities are expressed in units of m s^{-1}.

model to simulate TC maximum wind speeds greater than 45 m s^{-1}, recent research suggests that model errors in larger-scale features that affect the spatial distribution of TCs (e.g., the subtropical high) are likely not related to resolution [*Manganello et al*., 2012]. Additionally, we note that these errors do not necessarily explain the lack of modeled TC genesis over the Gulf of Mexico, which occurs for other climate models and may result from strong simulated wind shear and/or an insufficient model response to the Madden-Julian Oscillation.

Although it is clear that the FSU/COAPS model fails to reproduce the observed spatial distribution of per region maximum or limiting TC intensity, the ability of the model to capture the observed spatial distribution of per region *potential intensity* has not yet been examined. Here we compare per region potential intensity calculated from MERRA and FSU/COAPS atmospheric fields (Figure 6). Potential intensity calculated from MERRA data is referred to as observed potential intensity, although we acknowledge that the values were not truly "observed." Interestingly, while the model severely underestimates maximum and limiting intensity, it overestimates potential intensity. Despite this, the spatial distribution of modeled potential intensity compares much better with what we observe. When we examine scaled per region potential intensity, we find that regions with the highest observed potential intensity correspond to regions with the highest modeled potential intensity (Figure 6). Thus we conclude that although the model does not generate strong TCs, it does correctly simulate the environment necessary to support strong TCs.

When we compare per region maximum, potential, and limiting intensity for observed and model-generated TCs, we find that the FSU/COAPS model overestimates potential intensity by 2–10 m s^{-1} and underestimates maximum and limiting intensity by as much as 30 m s^{-1} (Figure 7). As expected, regions with the highest observed potential intensity correspond to regions with the highest observed maximum and limiting intensities. Additionally, regions with the highest potential intensity have a higher ratio of per region maximum intensity to potential intensity. In general, these regions occur over the Gulf of Mexico, which agrees with previous work by *DeMaria and Kaplan* [1994].

One explanation for the overestimation of potential intensity by the FSU/COAPS model is that the model yields cooler upper tropospheric temperatures relative to the MERRA reanalysis. *Emanuel et al.* [2013] explore the relationship between potential intensity and the tropical tropopause layer and suggest that cooling in this

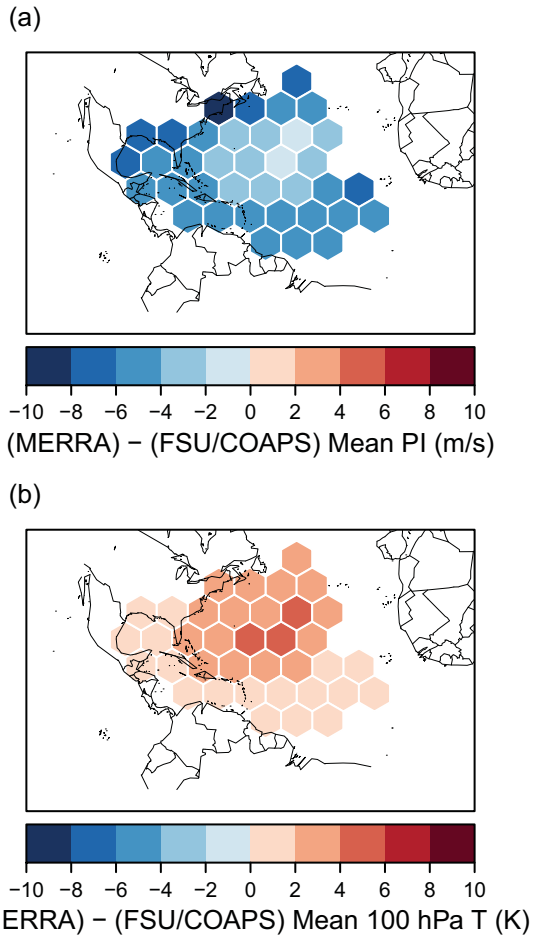

Figure 8. Difference maps displaying per region observed-modeled (MERRA—FSU/COAPS) mean August–October potential intensity (PI) in units of m s^{-1} (a), and per region observed-modeled mean August–October 100 hPa temperature in units of °C (b). Both temperature and potential intensity means are taken over the entire 1982–2008 time period. We include all regions that have either 15 observed TCs *or* 15 model-generated TCs.

layer is associated with increases in potential intensity. Indeed, modeled 100 hPa temperatures are consistently cooler than reanalyzed temperatures (Figure 8b). Interestingly, regions with the largest difference in observed versus modeled potential intensity (Figure 8a) correspond to regions with the smallest difference in 100 hPa temperature (Figure 8b). This suggests that tropopause temperature alone does not explain the overestimation of potential intensity by the FSU/COAPS model. The FSU/COAPS model tends to overestimate CAPE over the North Atlantic, which also results in higher simulated potential intensity.

5. The Sensitivity of Potential Intensity to SST

While previous research quantified the sensitivity of TC limiting intensity to SST for observed and GCM-generated TCs, the statistical relationship between potential intensity and SST has not been explored using the spatial tessellation approach. Here we use atmospheric fields from MERRA and the FSU/COAPS model to estimate potential intensity and then quantify the sensitivity of per region potential intensity to SST. Sensitivity is defined as the slope coefficient from the regression of maximum, limiting, or potential intensity onto August–October SST. To be consistent with previous research, we only consider regions with SST > 25°C. Over the 1982–2008 time period and using this specific set of regions, we find that the sensitivity of limiting intensity to SST is 7.1 m s^{-1} $°C^{-1}$ for observed TCs (Table 2), which compares well with previous estimates in *Elsner et al.* [2012b] who used slightly smaller regions. Similarly, the sensitivity of per region observed TC maximum intensity to SST is 7.2 m s^{-1} $°C^{-1}$. As with previous research, we find a statistically significant difference between the sensitivities of observed versus FSU/COAPS limiting intensity to SST (Figure 9). The sensitivities of FSU/COAPS limiting and maximum intensity to SST are not statistically different from zero (Table 2).

One possible explanation for this discrepancy is that the FSU/COAPS model resolution is too low to resolve the maximum wind speeds of TCs. Because of this, model-generated TCs are much weaker on average compared to observed TCs. Additionally, the sensitivity of model-generated TCs to SST may be affected by the lack of modeled TC activity over the Gulf of Mexico. The strongest observed TCs over this region occur over some of the warmest SSTs in the basin, leading to a high sensitivity. For a high sensitivity to exist, model-generated TCs must occur over a broad range of SSTs, with stronger TCs occurring over the warmest SSTs and weaker TCs occurring over the coolest SSTs. This does not occur for the FSU/COAPS model.

When we compare the sensitivity of observed TC maximum and limiting intensity to SST with the sensitivity of potential intensity to SST, the slopes of the three lines are statistically indistinguishable at the 95% confidence level (Figure 9). We estimate the sensitivity of potential intensity to SST to be 3.7 m s^{-1} $°C^{-1}$ when potential intensity is calculated from MERRA data (Table 2). Although this point estimate is slightly lower than our estimate for the sensitivity of limiting intensity to SST, the uncertainty bounds overlap at the 95% confidence level (Figure 9). This demonstrates that the observed statistical sensitivity of maximum/limiting

Table 2. Regressions of Three Measures of the Upper Limit of TC Intensity Onto SST[a]

Regression	Slope coefficient (m s^{-1}°C^{-1})	s.e.	t-Value	R^2
W_max ~ SST	7.2	0.998	7.24	0.686
W_max ~ SST (FSU/COAPS)	−0.15	0.954	−0.160	<0.001
PI ~ SST	3.8	0.334	11.4	0.845
PI ~ SST (FSU/COAPS)	3.6	0.439	8.28	0.733
LI ~ SST	7.1	0.967	7.32	0.691
LI ~ SST (FSU/COAPS)	3.5×10^{-3}	1.19	3.00×10^{-3}	<0.001

[a]We consider the per region maximum intensity (W_max), the per region maximum potential intensity (PI), and the per region limiting intensity (LI). The results displayed here regress the per region intensity measures onto the set of per region average August–October SST. We only consider those regions with August–October SST > 25°C. The first column lists the regression. The slope coefficient represents the sensitivity of TC maximum, limiting, or potential intensity to SST. The third column provides the standard error (s.e.) on the regression.

intensity to SST is approximately the same as the observed sensitivity of potential intensity to SST. Given this, if a model with a horizontal resolution of ~0.94° can capture the relationship between potential intensity and SST, then model simulations may still provide useful information about the upper limit of TC intensity even if they do not generate realistically intense TCs.

We find that while the FSU/COAPS model fails to capture the sensitivity of limiting or maximum intensity to SST, it successfully reproduces the sensitivity of observed potential intensity to SST (Figure 9). The model generates an environment conducive to the formation of strong TCs over the same regions that we observe strong TCs. This supports the notion that resolution inhibits the FSU/COAPS model from capturing the observed sensitivity of TC maximum and limiting intensity to SST. Other factors that are likely not related to model resolution, such as a lack of modeled TC activity over the Gulf of Mexico, may also affect the sensitivity.

Finally, we examine the spatial patterns of residuals from the regression of limiting intensity onto SST and the regression of potential intensity onto SST. Positive residuals indicate regions for which the regression underpredicts limiting intensity from SST, whereas negative residuals indicate regions of overprediction. Overall, residual patterns from the regressions of observed and modeled limiting intensity onto SST do not match (Figures 10a and 10b). For observed data, the regression tends to underpredict for regions in the western portion of basin. This area of underprediction is shifted into the central portion of the basin for modeled data. Although these residual patterns do not match, residuals from the regressions of modeled and observed *potential intensity* onto SST match relatively well (Figures 10c and 10d). Regions for which the

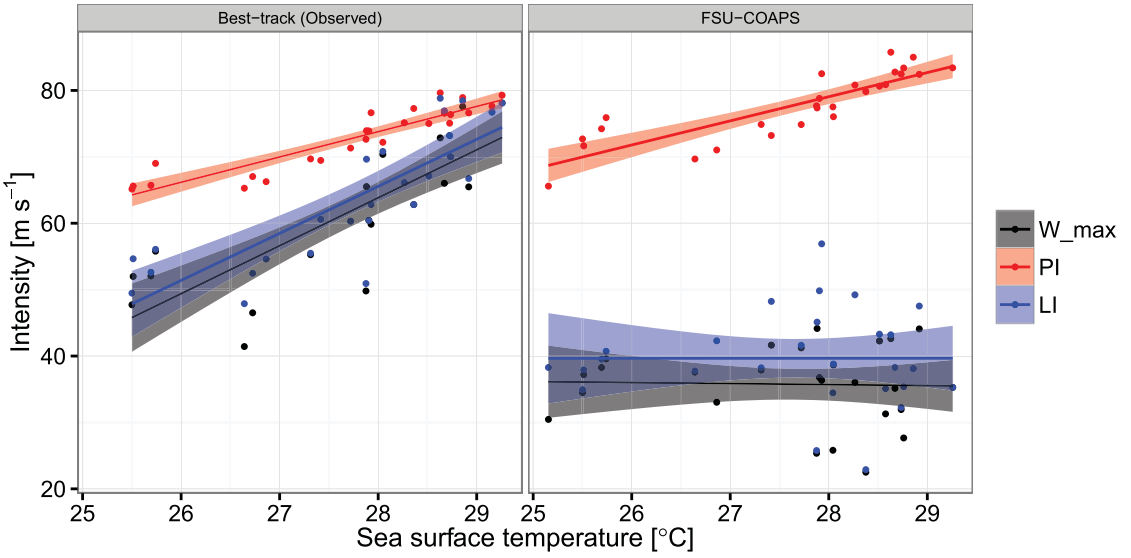

Figure 9. The sensitivity of per region maximum intensity (W_max; black), potential intensity (PI; red), and limiting intensity (LI; blue) to SST for observed (left) and model-generated (right) TCs. Each point represents the average August–October SST and the maximum, limiting, or potential intensity for a specific region. Shading indicates the 95% confidence interval about the regressions. Intensity metrics are expressed in units of m s^{-1} and SST is expressed in °C.

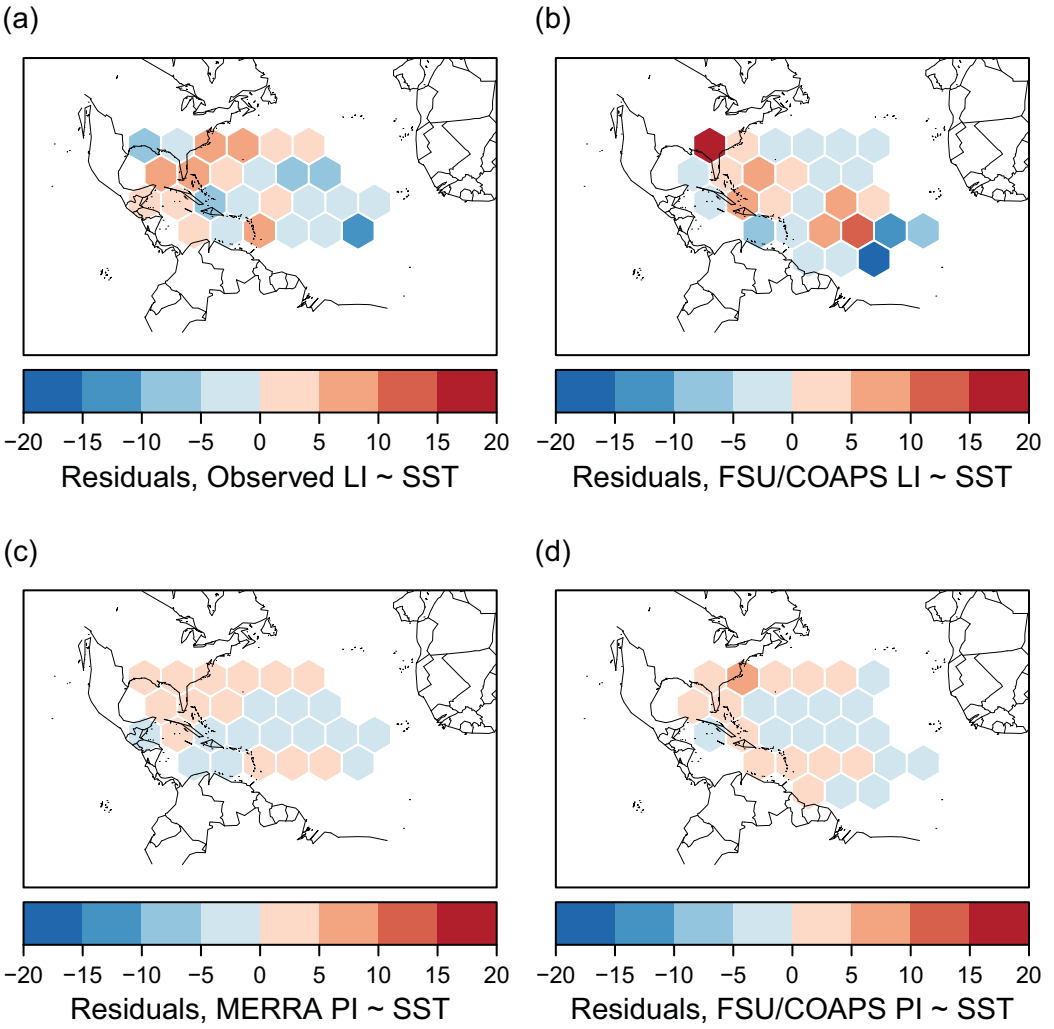

Figure 10. The spatial pattern of residuals from the regression of limiting intensity onto SST (LI ∼ SST) for observed (a) and modeled (FSU/COAPS; b) data. Bottom plots display residuals from the regression of potential intensity onto SST (PI ∼ SST) for observed (MERRA; c) and modeled (FSU/COAPS; d) data. Blue shading indicates regions of overprediction by the regression while red shading indicates regions of underprediction.

regression underpredicts observed potential intensity (e.g., Gulf of Mexico) correspond well with regions of underprediction of FSU/COAPS potential intensity.

6. Summary and Discussion

While previous research estimated the sensitivity of TC limiting intensity to SST for observations and two GCMs, no comparison had been made between the statistical limiting intensity and the physically derived potential intensity. Additionally, possible explanations for the much lower sensitivity of model-generated TCs relative to observed TCs had not been explored. The research presented here addresses both of these topics. We find that while the model fails to capture the spatial distribution of observed maximum or limiting intensity, it reproduces the observed spatial pattern of potential intensity reasonably well. However, the model does slightly overestimate per region potential intensity. This overestimation of potential intensity may be partially explained by cooler upper tropospheric temperatures in the model.

We also show that the sensitivity of observed limiting intensity to SST compares well with the sensitivity of potential intensity to SST. This result links the statistically defined limiting intensity to the physically defined potential intensity and supports the idea that the upper limit of TC intensity increases in concert with SST. This also suggests that if a GCM is able to reproduce the sensitivity of potential intensity to SST, model

simulations may still yield useful information about the upper limit of TC intensity even if they are unable to reproduce the distribution of observed TC intensity. Finally, results indicate that while the FSU/COAPS model is unable to reproduce the sensitivity of limiting intensity to SST, it captures the sensitivity of potential intensity to SST very well. The sensitivity of observed potential intensity to SST is 3.8 ± 0.334 m s^{-1} $°C^{-1}$ and the sensitivity of modeled potential intensity to SST is 3.6 ± 0.439 m s^{-1} $°C^{-1}$.

These results support the notion that low resolution inhibits the ability of climate models to generate realistic TCs. The suitable environment for strong TC development may exist, but strong simulated TCs do not form. Additionally, we show that the FSU/COAPS model does not generate or track as many TCs over the Gulf of Mexico as are observed. This may also affect the sensitivity of model-generated TC limiting intensity to SST because some of the warmest North Atlantic SSTs occur in this portion of the basin. To achieve a high sensitivity, model-generated TCs must occur over a broad range of SSTs, with stronger TCs occurring over the warmest SSTs and weaker TCs occurring over the coolest SSTs. If very few (and very weak) model-generated TCs occur over the warmest water, then the sensitivity of modeled limiting intensity to SST will not be high. Previous research suggests that improved resolution will not necessarily rectify model errors associated with the spatial distribution of TCs. It is possible that different convective parameterization schemes may yield different results for TCs over the Gulf of Mexico. More research is necessary to address these issues. Additionally, future research will explore the sensitivity of TC intensity metrics to SST for a broader suite of GCMs, including those with significantly higher spatial resolution.

Acknowledgments

Grant support for this research came from the Risk Prediction Initiative (JBE), the U.S. Department of Energy Office of Science (TEL), and the NOAA Climate Program Office (TEL). Observed tropical cyclone data used in this paper can be obtained at http://www.nhc.noaa.gov/data/#hurdat. The code used to interpolate the TC data can be found at http://www.hurricaneclimate.com/. SST data were obtained from http://www.esrl.noaa.gov/psd/data/gridded/data.noaa.ersst.html, and MERRA reanalysis data were downloaded from http://disc.sci.gsfc.nasa.gov/mdisc/data-holdings/merra/merra_products_nonjs.shtml. Finally, FSU/COAPS model data were provided by Tim LaRow (tlarow@fsu.edu). All of the code used to generate these results can be found at http://rpubs.com/sestrazz/55292.

References

Bender, M. A., T. R. Knutson, R. E. Tuleya, J. J. Sirutis, G. A. Vecchi, S. T. Garner, and I. Held (2010), Modeled impact of anthropogenic warming on the frequency of intense Atlantic hurricanes, *Science*, *327*, 454–458.

Braun, M. A., J. A. Sippel, and D. S. Nolan (2012), The impact of dry midlevel air on hurricane intensity in idealized simulations with no mean flow, *J. Atmos. Sci.*, *69*(1), 236–257.

Chen, S. S., W. Zhao, M. A. Donelan, J. F. Price, and E. J. Walsh (2007), The CBLAST-Hurricane Program and the next-generation fully coupled atmosphere-wave-ocean models for hurricane research and prediction, *Bull. Am. Meteorol. Soc.*, *88*, 311–317.

Cocke, S. D., and T. E. LaRow (2000), Seasonal predictions using a regional spectral model embedded within a coupled ocean-atmosphere model, *Mon. Weather. Rev.*, *128*, 689–708.

DeMaria, M. (1996), The effect of vertical shear on tropical cyclone intensity change, *J. Atmos. Sci.*, *53*(14), 2076–2087.

DeMaria, M., and J. Kaplan (1994), Sea surface temperature and the maximum intensity of Atlantic tropical cyclones, *J. Clim.*, *7*(19), 1324–1334.

Elsner, J. B., and T. H. Jagger (2013), *Hurricane Climatology: A Modern Statistical Guide Using R*, 390 pp., Oxford Univ. Press, N. Y.

Elsner, J. B., J. P. Kossin, and T. H. Jagger (2008), The increasing intensity of the strongest tropical cyclones, *Nature*, *455*(7209), 92–95.

Elsner, J. B., R. E. Hodges, T. H. Jagger (2012a), Spatial grids for hurricane climate research, *Clim. Dyn.*, *39*, 21–36.

Elsner, J. B., J. C. Trepanier, S. E. Strazzo, and T. H. Jagger (2012b), Sensitivity of limiting hurricane intensity to ocean warmth, *Geophys. Res. Lett.*, *39*, L17702, doi:10.1029/2012GL053002.

Elsner, J. B, S. E. Strazzo, T. H. Jagger, T. LaRow, and M. Zhao (2013), Sensitivity of limiting hurricane intensity to SST in the Atlantic from observations and GCMs, *J. Clim.*, *26*(16), 5949–5957.

Emanuel, K. A. (1987), The dependence of hurricane intensity on climate, *Nature*, *326*(61112), 483–485.

Emanuel, K. A. (1995), Sensitivity of tropical cyclones to surface exchange coefficients and a revised steady-state model incorporating eye dynamics, *J. Atmos. Sci.*, *52*(22), 3969–3976.

Emanuel, K. A. (2005), Increasing destructiveness of tropical cyclones over the past 30 years, *Nature*, *436*(7051), 686–688.

Emanuel, K. A. (2013), Downscaling CMIP5 climate models shows increased tropical cyclone activity over the 21st century, *Proc. Natl. Am. Sci. U. S. A.*, *110*(30), 12,219–12,224.

Emanuel, K. A., S. Solomon, D. Folini, S. Davis, and C. Cagnazzo (2013), Influence of tropical tropopause layer cooling on Atlantic hurricane activity, *J. Clim.*, *26*(7), 2288–2301.

Evans, J. L. (1993), Sensitivity of tropical cyclone intensity to sea surface temperature, *J. Clim.*, *6*(6), 1133–1140.

Held, I. M., and M. Zhao (2011), The response of tropical cyclone statistics to an increase in CO2 with fixed sea surface temperatures, *J. Clim.*, *24*(20), 5353–5364.

Jarvinen, B. R., C. J. Neumann, and M. A. S. Davis (1988), A tropical cyclone data tape for the North Atlantic basin, 1886–1983: Contents, limitations and uses, *NOAA Tech. Mem, NWS NHC 22*, 21 pp., NWS NHC, Coral Gables, Fla.

Knutson, T. R., J. J. Sirutis, S. T. Garner, G. A. Vecchi, and I. M. Held (2008), Simulated reduction in Atlantic hurricane frequency under twenty-first-century warming conditions, *Nat. Geosci.*, *1*(6), 359–364.

Knutson, T. R., et al. (2013), Dynamical downscaling projections of twenty-first-century Atlantic hurricane activity: CMIP3 and CMIP5 model-based scenarios, *J. Clim.*, *26*(17), 6591–6617.

Kossin, J. P. (2015), Validating atmospheric reanalysis data using tropical cyclones as thermometers, *Bull. Am. Meteorol. Soc.*, in press, doi:10.1175/BAMS-D-14_00180.1.

Kunkel, K. E., et al. (2013), Monitoring and understanding trends in extreme storms: State of knowledge, *Bull. Am. Meteorol. Soc.*, *94*(4), 499–514.

LaRow, T. E., Y. K. Lim, D. W. Shin, E. P. Chassignet, and S. D. Cocke (2008), Atlantic Basin Seasonal Hurricane Simulations, *J. Clim.*, *21*, 3191–3206.

LaRow, T. E., L. Stefanova, and C. Seitz (2014), Dynamical simulations of north Atlantic tropical cyclone activity using observed low-frequency SST oscillation imposed on CMIP5 Model RCP4. 5 SST projections, *J. Clim.*, *27*(21), 8055–8069.

Levitus, S., J. I. Antonov, T. P. Boyer, and C. Stephens (2000), Warming of the world ocean, *Science*, *287*(5461), 2225–2229.

Levitus, S., et al. (2012), World ocean heat content and thermosteric sea level change (0–2000 m), 1955–2010, *Geophys. Res. Lett.*, *39*, L10603, doi:10.1029/2012GL051106.

Manganello, J. V., et al. (2012), Tropical cyclone climatology in a 10-km global atmospheric GCM: Toward weather-resolving climate modeling, *J. Clim.*, *25*(11), 3867–3893.

Merrill, R. T. (1987), An experiment in statistical prediction of tropical cyclone intensity change, *NOAA Tech. Mem.*, *NWS NHC-34*, 34 pp., NWS NHC.

Rayner, N. A., D. E. Parker, E. B. Horton, C. K. Folland, L. V. Alexander, D. P. Powell, E. C. Kent, and A. Kaplan (2003), Global analyses of sea surface temperature, sea ice, and night marine air temperature since the late nineteenth century, *J. Geophys. Res.*, *108*(D14), 4407, doi: 10.1029/2002JD002670.

Rienecker, M. M., et al. (2011), MERRA: NASA's modern-era retrospective analysis for research and applications, *J. Clim.*, *24*(14), 3624–3648.

Smith, T. M., T. W. Reynolds, T. C. Peterson, and J. Lawrimore (2008), Improvements to NOAA's historical merged land-ocean surface temperature analysis (1880–2006), *J. Clim.*, *21*(10), 2283–2296.

Strazzo, S., J. B. Elsner, T. LaRow, D. J. Halperin, and M. Zhao (2013a), Observed versus GCM-generated local tropical cyclone frequency: Comparisons using a spatial lattice, *J. Clim.*, *26*(21), 8257–8268.

Strazzo, S., J. B. Elsner, J. C. Trepanier, and K. A. Emanuel (2013b), Frequency, intensity, and sensitivity to sea-surface temperature of North Atlantic TCs in best-track and simulated data, *J. Adv. Model. Earth Syst.*, *5*, 500–509, doi:10.1002/jame.20036.

Vecchi, G. A., S. Fueglistaler, I. M. Held, T. R. Knutson, and M. Zhao (2013), Impacts of atmospheric temperature trends on tropical cyclone activity, *J. Clim.*, *26*(11), 3877–3891.

Villarini, G., and G. A. Vecchi (2013), Projected increases in North Atlantic tropical cyclone intensity from CMIP5 models, *J. Clim.*, *26*(10), 3231–3240.

Walsh, K. J. E., et al. (2015), Hurricanes and climate: The US CLIVAR working group on hurricanes, *J. Clim.*, in press, 10.1175/BAMS-D-13-00242.1.

Wong, M. L. M., and J. C. L. Chan (2004), Tropical cyclone intensity in vertical wind shear, *J. Atmos. Sci.*, *61*(15), 1859–1876.

Zhao, M., I. M. Held, S. J. Lin, and G. A. Vecchi (2009), Simulations of global hurricane climatology, interannual variability, and response to global warming using a 50-km resolution GCM, *J. Clim.*, *22*(24), 6653–6678.